



Cardiac Malformations in EMILIN2 Deficient Mice

Anuradha Guggilam¹, Devaraja Sannanngiah^{2,5}, Yanqing Gong^{2,6}, Jessica Grondolsky², Menggui Huang^{2,7}, Huigin Nie², Elaine C Davis³, Yehe Liu⁴, Michael Jenkins⁴, James Strainic⁴ and Jane Hoover-Plow^{1,2*}

Abstract

Background: EMILIN2, elastin microfibril interface located protein 2, is expressed during cardiovascular development, by cardiac stem cells, and in adult animal models of heart disease. In humans, the EMILIN2 gene is located on the short arm of Chromosome 18, and patients with partial or complete deletions of this chromosome region have cardiac malformations. The objective of this study was to evaluate whether the Emilin2 deficient mice have cardiac defects.

Methods and results: Cardiac malformations were assessed in adult Emilin2, Emilin1 (EMILIN2 homologue) deficient mice, and Emilin2:Emilin1 double deficient mice. The primary malformation in Emilin2 deficient mice was ventricular septal defects. Although EMILIN1, is also expressed during cardiovascular development, the primary cardiac anomalies in Emilin1 deficient mice were valve insufficiency (pulmonary, aortic and mitral). Only half of the expected Emilin2:Emilin1 double deficient offspring were weaned, indicating embryonic and perinatal lethality. Surviving Emilin2:Emilin1 double deficient mice had both ventricular septal defects and regurgitation of valves. There was a trend for anterior wall thinning and left ventricular dilation in Emilin2:Emilin1 double deficient mice. In embryonic Emilin2:Emilin1 double deficient mice complete arterioventricular canal defects and ventricular septal defects were identified. A potential mechanism for development of cardiac defects in Emilin2 deficiency may be reduced mobilization of stem cells during heart development.

Conclusions: Emilin2 deficient mice express cardiac anomalies, primarily ventricular septal defects, and Emilin1 mice exhibit primarily valve abnormalities including pulmonary regurgitation, whereas in Emilin2: Emilin1 double deficient mice, both anomalies occurred, suggesting that Emilin2 and Emilin1 have differential roles in cardiac development. Emilin2 deficient mice have cardiac malformations similar to individuals with deletions of the short arm of Chromosome 18. Emilin2 deficient mice may be an informative model to investigate the consequences of cardiac anomalies in subjects with deletions of the short arm of Chromosome 18, 18p.

Keywords

Emilin2 deficiency; Emilin1 deficiency; Cardiac malformations; Ventricular septal defects; Pulmonary regurgitation; Optical coherence tomography

Introduction

Deletion of 18p is one of the most common chromosomal deletion syndromes with an incidence of about 1:50,000 births [1,2]. A recent study found that 56% of 18p subjects have documented cardiac defects [3]. Heart malformations reported in several studies include tetralogy of Fallot, pulmonary valve stenosis, mitral valve prolapse, aortic coarctation, VSDs, and aortic stenosis [4-15]. However, the identity of the causative gene of the cardiac anomalies in the 18p deletion subjects is unknown. There are 67 known genes [3] in the 18p region, but only a few of these genes have been implicated with the clinical symptoms. *TGIF* [16], and *HPE4* [17] have been associated with the holoprosencephaly, *DYT7* with the dystonia [18], *SMCHD1* [19] with the facioscapulohumeral muscular dystrophy type 2, and a locus for susceptibility to alopecia [20]. However, none of the known genes in 18p have been associated with cardiac malformations.

Emilin2 (E2) is expressed in the cardiovascular system during development in the mouse [2,21,22] and zebra fish [23]. Studies [11,24] in mice reported that E2 is differentially expressed in right ventricular tissue. The goal of this study was to investigate whether E2 deficient (*E2*^{-/-}) mice also had cardiac defects.

E2 was first identified as a binding partner to Emilin1 (E1), and both are elastin microfibril interface located proteins. E2 is highly homologous to E1, with 70% homology in their N-terminal and 75% in their C-terminal domains [25]. Recently, Bot et al. [26] reported multiple interactions among E2 and E1 N-terminal and C-terminal domains, suggesting possible homo- and hetero-multimer interactions. Differential expression of E1 and E2 has been reported in both mouse [2] and zebra fish [23]. In adult mice we reported expression of E2 in the aorta and heart [27] and expression of E1 has been reported in both human and mouse heart valves [28-30].

Here we report that *E2*^{-/-} mice express right-sided heart defects, whereas E1 deficient (*E1*^{-/-}) mice exhibit primarily valve abnormalities including pulmonary regurgitation, double deficient mice, *E2*^{-/-}:*E1*^{-/-} exhibit both VSDs and pulmonary regurgitation, suggesting that E1 and E2 have differential roles in cardiac development.

Materials and Methods

Mice

E2^{-/-} mice were generated in a C57BL/6 (B6) background with two lox-P sites flanking exon 3 in the mouse genome (Taconic) and previously described [31]. *E2*^{lox/lox} mice were crossed with the CMV-Cre recombinant mice to generate global *E2*^{-/-} mice. *E2*^{-/-} mice were compared to wild-type mice with CMV-Cre (WTc). Professor Giorgio Bressan, University Padua, Italy, kindly provided *E1*^{-/-} mice in a B6 background and B6 mice were used as the control (WT) for *E1*^{-/-} mice. The expected number of 25% wildtype, 50% heterozygous, and 25% deficient mice were found in *E1*^{-/-} and *E2*^{-/-} mice, suggesting no embryonic lethality in the single deficient mice. *E2*^{-/-} and *E1*^{-/-} mice were bred to obtain heterozygous mice, genotyped and bred to generate homozygous *E2*^{-/-}:*E1*^{-/-} mice. The phenotype of the *E2*^{-/-}:*E1*^{-/-} was expected to be more severe than either of the single deficient mice, and indeed only 50% (12% rather than the 25%) of the expected offspring (from *E2*^{+/-} X *E1*^{+/-} breeding pairs) survived to weaning. All

*Corresponding author: Jane Hoover-Plow, PhD, Department of Molecular Cardiology, NB5 Cleveland Clinic Lerner Research Institute 9500 Euclid Avenue, Cleveland, OH 44195, USA, Tel: (216)445-8207; Fax: (216)444-8204; E-mail: hooverj@ccf.org

Received: June 06, 2016 Accepted: September 07, 2016 Published: September 12, 2016

mice were maintained on B6 background and utilized at 8-10 weeks of age. Mice were bred, housed in sterilized isolator cages, maintained on a 14-hour light/10-hour dark cycle, and provided with sterilized food and water at the Biological Resource Unit of the Cleveland Clinic Lerner Research Institute. All animal experiments were performed in accordance with protocols approved by the Cleveland Clinic Institutional Animal Research Committee.

Ultrasound imaging and doppler echocardiography

Mice were sedated with 1-2% isoflurane and echocardiography was performed using the GE Vivid7 with a 14-MHz i13L transducer for cardiac phenotyping. Color flow and spectral doppler imaging were obtained to detect any cardiac anomalies. Briefly, left ventricular (LV) dimensions were quantified by digitally recorded 2D clips and M-mode images in a short axis view from the mid-LV just below the papillary muscles to allow for consistent measurements from the same anatomic location in different mice. Ejection fraction (EF), percent fractional shortening (%FS), heart rate (HR), anterior wall thickness in systole (AWTs), left ventricle internal diameter in systole (LVIDs) measurements were made. All studies were performed on awake mice. After cardiac perfusion, the aortas were harvested, immediately embedded into OCT (Tissue-Tek, Torrance, CA) and frozen. The frozen aortas were sectioned at 10 μ m using a cryostat (Leica CM1850, Leica Microsystems, Nassloch, Germany) and stained with Hematoxylin and Eosin (H&E).

Structural imaging using optical coherence tomography

Optical coherence tomography (OCT) has been previously shown as an effective tool for 3-D structural imaging of embryonic cardiac tissues [32-35]. In this study, 7 $E2^{-/-}$ embryonic mouse hearts were collected at E19.5. The hearts were fixed in 4% paraformaldehyde with 1X phosphate buffered saline (PBS) overnight under room conditions, followed by 3 consecutive 10 min rinsing sessions in 1X PBS. To reduce light scattering and increase imaging depth, optical clearing has been utilized in combination with 3-D imaging to visualize the morphology of the heart without sectioning the tissue [34-37]. In this experiment, the fixed hearts were cleared in excess *Sca/eCUBIC-1* optical clearing reagent containing 25 wt% Urea, 25 wt% N,N,N',N'-tetrakis(2-hydroxypropyl) ethylenediamine, 15 wt% Triton X-100 and 35 wt% deionized water. The hearts were cleared for 3 days at room temperature while being shaken at 200 rpm [38]. The cleared hearts were then imaged using a custom-built spectral domain OCT system [39], with the cleared tissue immersed in the original optical clearing reagent for optimized refractive index matching. The OCT system used in this study employs a 1300 \pm 50 nm superluminescent diode, a quasi-telecentric galvo scanner, a prism based linear-wavenumber spectrometer and a line-scan camera with variable line rate. Both the lateral and the axial resolution of the OCT system is about 10 μ m in the cleared tissue. Custom Matlab (MathWorks; Natick, MA) programs were employed to process the images from the raw binary data collected from the OCT system. The 3-D datasets were then inspected by an experienced fetal echocardiography investigator to determine phenotype abnormalities. Slice and volume images of the hearts were rendered and visualized using a commercial visualization program called Amira (FEI Visualization Sciences Group; Burlington, MA).

Results

Congenital heart defects in $E2^{-/-}$, $E1^{-/-}$ and $E2^{-/-};E1^{-/-}$ mice

Cardiac anomalies were detected by color Doppler flow recordings

in $E2^{-/-}$, $E1^{-/-}$ and $E2^{-/-};E1^{-/-}$ mice. Color flow Doppler echocardiography, in which flow movement toward the transducer is shown in red and flow movement away from the transducer is shown in blue, 2D-images from a modified short axis and apical 4-chamber views are shown in Figure 1. Ventricular septal defects (VSDs) were observed in these mice. Figure 1A shows sequential 2D echocardiography images of a representative $E2^{-/-}$ heart with VSD in apical 4-chamber view. VSD in both the 2D structural image (Figure 1Aa) and the doppler flow images are shown in Figure 1Ab-d. The incidence of VSDs in $E2^{-/-}$ mice was 56%, 33% in $E1^{-/-}$ mice, and 52% in the $E2^{-/-};E1^{-/-}$ double deficient mice compared to only 9% in CMV-Cre (WTc) mice (Table 1). There was no difference in heart to body weight ratio (Table 1) among the different strains.

Additionally, in $E2^{-/-}$ mice, stenotic flow patterns were captured as red, blue, and yellow mosaic patterns at the pulmonic and aortic valves during systole. The incidence of pulmonary regurgitation (PR) was only 7% in $E2^{-/-}$ mice compared to 56% in $E1^{-/-}$ mice, and in the double deficient mice, $E2^{-/-};E1^{-/-}$ 43%. Mice with the *E1* deficiency, $E1^{-/-}$ and $E2^{-/-};E1^{-/-}$ mice, had a >2-fold higher (56 & 43%) incidence of PR than mice with the *E1* gene *B6*, WTc, and $E2^{-/-}$ mice (10, 18 & 17). The CMV-Cre (WTc) mice had only 18% PR. $E1^{-/-}$ mice (Figure 1) had mitral regurgitation (MR) and aortic regurgitation (17%) (Table 1). Shown in the bottom panel of Figure 1C are thickened leaflets of the pulmonary and mitral valves (H&E staining). $E2^{-/-};E1^{-/-}$ mice also had mitral regurgitation (26%) and aortic regurgitation (9%) (Table 1). In Figure 1 in one $E2^{-/-};E1^{-/-}$ mouse the top panel shows the ascending aorta in a 2D long axis and the lower panel shows coarctation of the aorta.

Cardiac anomalies in embryonic $E2^{-/-}$ mice

Cardiac anomalies in E19.5 mouse hearts (Figure 2) were detected by 3D structural imaging using optical coherence tomography that is an effective tool for detecting cardiac abnormalities compared to traditional histochemistry. Of the 7 $E2^{-/-}$ fetal hearts evaluated, there was 2 out of 7 incidence of VSDs and 2 out of 7 had complete atrioventricular canal defects (CAVC) with abnormal great artery position. The $E2^{-/-}$ fetal hearts also exhibited hypoplastic right ventricles (HRV; 5 out of 7 incidence) and hypoplastic pulmonary arteries (HPA; 2 out of 7 incidence). Only 1 of the evaluated $E2^{-/-}$ fetal hearts were completely normal with no cardiac defects while 6 out of 7 exhibited one or more of the above described abnormalities.

Cardiac function

To determine whether the cardiac abnormalities altered cardiac function echocardiography was performed in these mice. Ejection fraction (Figure 3A) and percent fractional shortening (Figure 3B) were not different among the strains suggesting these cardiac defects did not alter systolic function in these mice. There was a trend for anterior wall thinning (Figure 3C) and left ventricular dilation (Figure 3D) in the $E2^{-/-};E1^{-/-}$ mice.

Potential mechanisms for the development for the cardiac anomalies in $E2^{-/-}$ mice

Four potential mechanisms for the cardiac anomalies in $E2^{-/-}$ mice were investigated: 1) abnormal platelet aggregation 2) abnormal blood vessel structure; 3) TGF- β 1 processing and 4) abnormal stem cell mobilization. In a previous study [31], we generated double deficient mice, in the C57BL/6J background. In this group of mice we selected mice with no cardiac defects, mice with pulmonary regurgitation, and

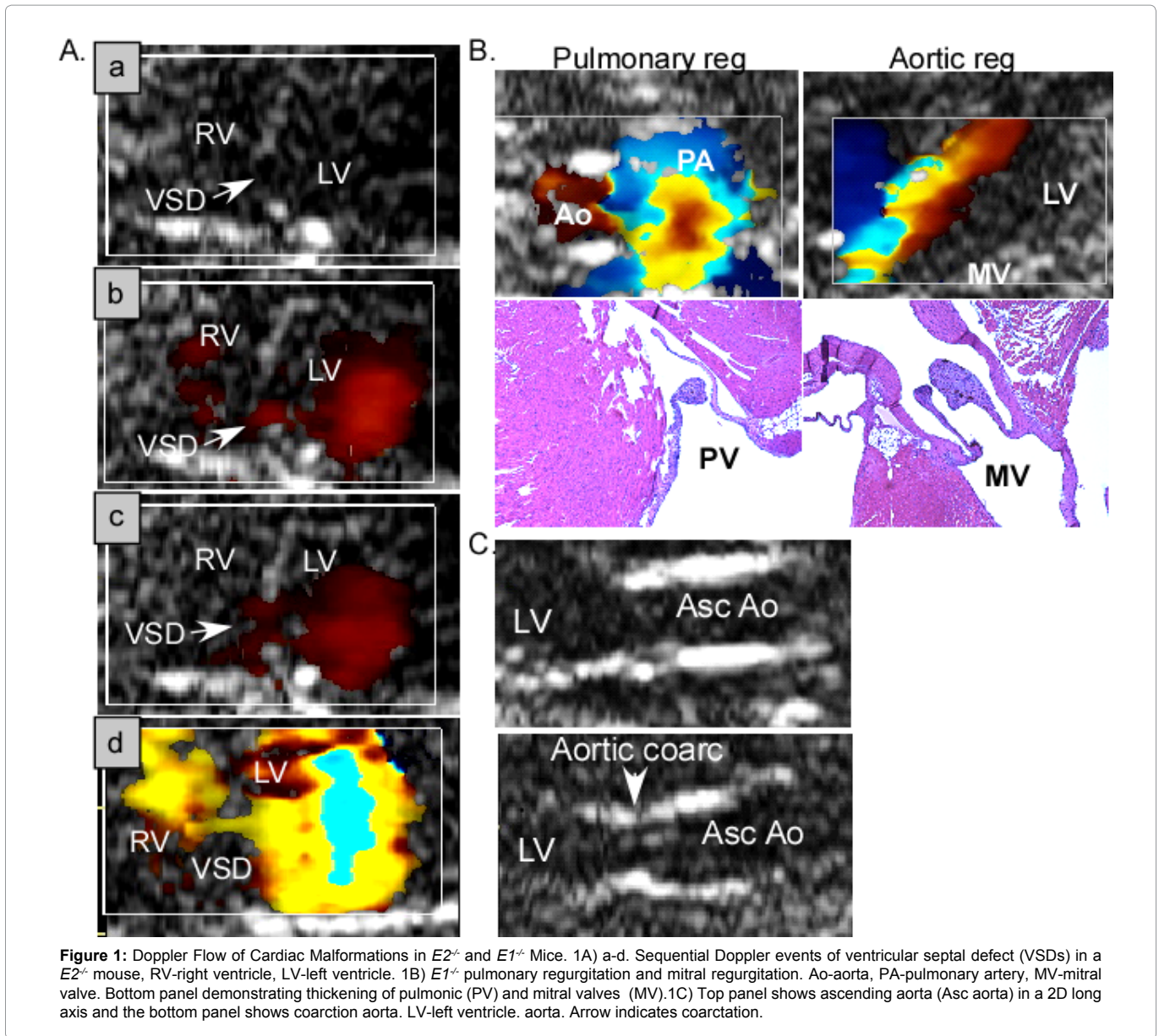


Table 1: Cardiac Anomalies in $E2^{-/-}$, $E1^{-/-}$, and $E2^{-/-};E1^{-/-}$ Mice.

Genotype	PR	AR	MR	VSDs	Heart/BWT (%)
B6	2/20 (10)	0/20 (0)	1/20(0)	0/20 (0)	0.58 ± 0.01
WTc	2/11 (18)	0/11 (0)	2/11 (18)	1/11 (9)	0.54 ± 0.17
$E2^{-/-}$	3/18 (17)	0/18 (0)	1/18 (6)	10/18 (56)	0.55 ± 0.32
$E1^{-/-}$	10/18 (56)	3/18(17)	3/18 (17)	6/18 (33)	0.58 ± 0.04
$E2^{-/-};E1^{-/-}$	10/23 (43)	2/23 (9)	6/23 (26)	12/23 (52)	0.59 ± 0.02

Number in parenthesis-% mice with defect; PR-pulmonary regurgitation; AR: Aortic Regurgitation; MR-Mitral Regurgitation; VSDs-Ventricular Septal Defect; Heart/BWT-% Heart Weight (g)/Body Weight.

mice with ventricle septal defects. Platelet aggregation, expressed as %maximum amplitude, was determined and there was no significant difference (one-way ANOVA) among the mice (n=3) with no defects (45 ± 1), pulmonary regurgitation and ventricle septal defects (38 ± 6), or mice with only ventricle suggesting platelet aggregation was

not altered in adult mice with cardiac defects septal defects (36 ± 3). Similar to the previous study, (31) we found that platelet aggregation in control mice (C57BL/6) was 71 ± 3 and was significantly different (p<0.001) than $E2^{-/-};E1^{-/-}$ mice as determined by a Dunnett's multiple comparison test.

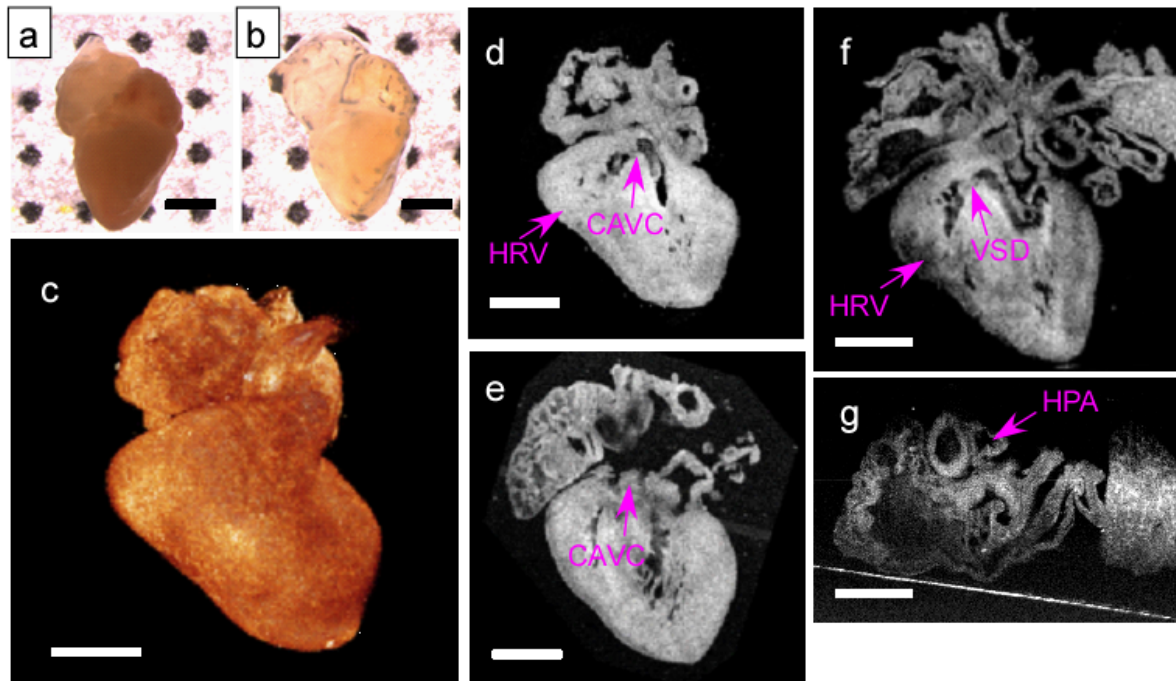


Figure 2: Stereomicroscopic and OCT images of selected $E2^{-/-}$ embryonic 19.5 day (E19.5) fetal mouse hearts. (All scale bars=1 cm) a) A stereomicroscopic image of a fixed heart sample before optical clearing. b) A stereomicroscopic image of the same heart sample in a) after being treated with a sca/eCUBIC-1 reagent for 3 days. Imaging was taken with identical illumination as in a), showing significantly improved transmission of light and similar tissue size c) 3-D rendered OCT image of a different $E2^{-/-}$ E19.5 heart showing abnormal exterior structure. d) 4-chamber view, cross-sectional image of the same heart in c) showing hypoplastic right ventricle (HRV) and possible complete atrioventricular canal defect (CAVC). e) 4-chamber view of a different $E2^{-/-}$ E19.5 heart showing CAVC. f) 4-chamber view of another $E2^{-/-}$ E19.5 heart showing HRV and a possible ventricular septal defect (VSDs). g) axial view of the same heart in f) showing a hypoplastic pulmonary artery (HPA).

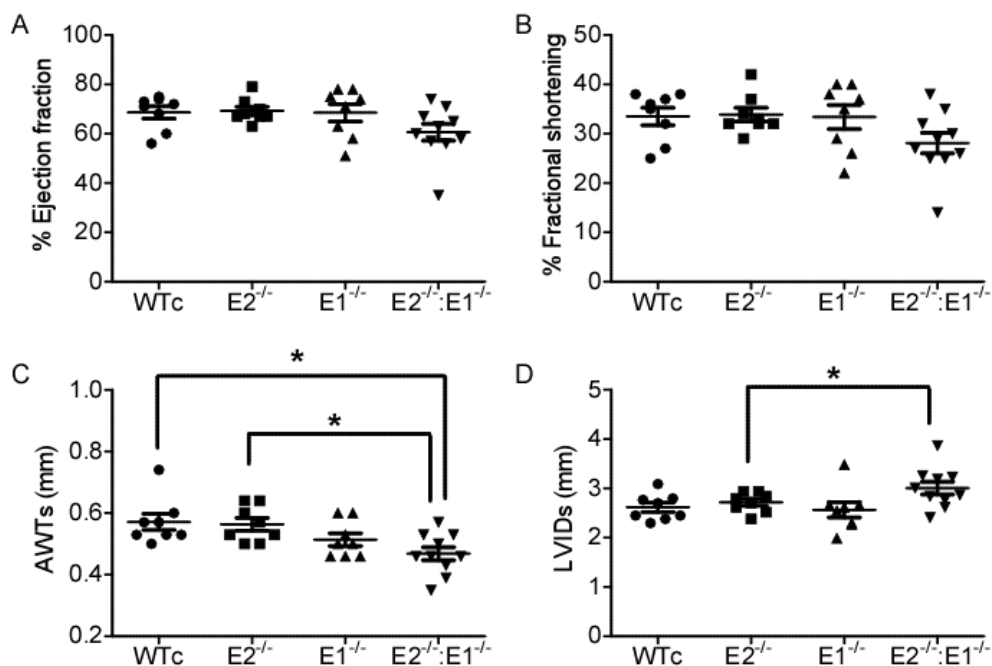


Figure 3: Echocardiography of $E2^{-/-}$, $E1^{-/-}$, $E2^{-/-}:E1^{-/-}$. A. Ejection Fraction (EF %); B. Fractional Shortening (FS%); C. Anterior Wall Thickness in Systole (AWTs, mm); D. Left Ventricular Internal Diameter in Systole (LVIDs, mm). Each mouse indicated with dot. Line is mean \pm SEM, n=8-10. Statistical analysis, Kruskal-Wallis test, Dunn's Multiple Comparison post-test, *p<0.05.

Unlike the *E1^{-/-}* mice [40], we did not detect any alterations in the elastic laminae, vascular smooth muscle cells or collagen (Supplementary Figure 1) of the aortic wall. The aorta wall consists of several layers [41-44] including endothelial cells, smooth muscle, elastic laminae, and collagen with specific attachments. In the *E1^{-/-}* mice the elastic laminae is disrupted and irregular compared to the elastic laminae in the *E1^{+/+}* mice (40). The arrangement of the layers and integrity of aorta were intact in the *E2^{-/-}* mice. In addition, after treatment with CaCl_2 to induce dilation, we did not find any difference in WTc (0.17 ± 0.02 mm) and *E2^{-/-}* (0.18 ± 0.03 mm) mice abdominal aortic diameter changes (post minus pre mm). Thus, in *E2^{-/-}* mice we did not find defects in the vessel wall that replicate the disrupted elastic laminae found in the aorta of the *E1^{-/-}* mice [40].

TGF- β 1 is important in cardiac development and recovery from injury [45,46]. E1 inhibits TGF- β 1 processing and a deficiency of E1 causes an increase in TGF- β 1. At the same age as plasma was collected, we measured heart TGF- β 1 mRNA and TGF- β 2 mRNA expression. There was no difference in TGF- β 1 or TGF- β 2 mRNA expression between the *E2^{-/-}* mice and WTc mice (Supplementary Figure 2A, B). In plasma (PPP) (Supplementary Figure 2C) from *E2^{-/-}*, *E1^{-/-}*, and *E2^{-/-}:E1^{-/-}* mice, total (latent plus activated) TGF- β 1 was elevated compared to B6, (*E2^{+/+}* and *E1^{+/+}*) mice (Supplementary Figure 2D). In the platelet rich plasma (PRP), a measure of TGF- β 1 platelet content, total (latent plus activated) TGF- β 1 was not different in platelets from *E2^{-/-}* or *E1^{-/-}* mice compared to the B6 mice. Since TGF- β 1 synthesis was not different in B6 and *E2^{-/-}* mice, the increase of TGF- β 1 in the plasma suggests that processing may be enhanced without E2 similar to that found in the *E1^{-/-}* mice.

E2 is found on the surface of stem cells and has been a useful marker to detect cardiac stem cells [47], but the function is not known. Granulocyte colony stimulating factor (G-CSF) mobilizes stem cells from the bone marrow and stem cells in the heart to sites of injury after a myocardial infarction [48] and during embryonic development [49]. We tested whether E2 deficiency would alter the mobilization of bone marrow WBC (Supplementary Figure 3A) and stem cells (Lin⁻kit⁺) after treatment with G-CSF (Supplementary Figure 3B). There was no difference in circulating WBC or hematopoietic stem cells in saline treated mice, but the response to G-CSF was 2-3-fold higher in the WT mice than *E2^{-/-}* mice indicating that E2 is necessary for stem cell mobilization.

Discussion

The results of this study show that 1) E2 deficiency causes right-sided heart defects; 2) E2 deficiency does not disrupt the aortic elastic lamina; 3) E2 deficiency results in increased plasma TGF- β 1; and 4) *E2^{-/-}* mice have impaired stem cell mobilization. The malformations in the *E2^{-/-}* mice were associated with defects in the cardiac septal and right ventricular walls of the heart, whereas the malformations in the *E1^{-/-}* mice were associated with the valves. These marked differences between the *E2^{-/-}* and *E1^{-/-}* mice in the expression of the cardiac malformations may be due to the temporal and spatial expression of the E2 and E1 during development. During early embryonic development in the mouse [2], E2 is strongly expressed in the neural fold, limb buds, and heart, whereas E1 shows a widespread expression in mesenchymal cells in the head and trunk. In E14.5-old mouse embryos; E2 is expressed in the trabecular zone of the heart ventricle and many mesenchymal cells. E1 is found in the mesenchymal cells throughout the body, and in the outflow tract at the aortic trunk and aortic valve [2].

Another difference between *E2^{-/-}* and *E1^{-/-}* mice is that the structure of the aorta is disrupted in the *E1^{-/-}* mice (40, 44), but not in the *E2^{-/-}* mice. Also, we found no difference in abdominal aortic aneurysm formation in *E2^{-/-}* mice at 8-10 weeks of age compared to WTc controls. Changes may occur in the aorta and the abdominal aortic aneurysm formation in older *E2^{-/-}* mice. Munjal et al. [30] recently reported a progression of the aortic valve disease in the older *E1^{-/-}* mice with age (12-14 months) compared to young mice (8-10 days).

Mutations in the TGF- β 1 pathway have been shown to contribute to the occurrence of congenital VSDs [50-54]. TGF- β 1 was increased in *E2^{-/-}* mice, suggesting that *E2^{-/-}* mice may be important in the regulation of TGF- β 1 processing. E1 was identified as an inhibitor and regulator of the furin-processing step of TGF- β 1 [55,56]. In *E1^{-/-}* mice, furin processing is not inhibited by E1 and thus, more TGF- β 1 is available for further processing and enhanced signaling. TGF- β 1 and TGF- β 2 mRNA expression was not elevated in the heart of the *E2^{-/-}* mice, but TGF- β 1 in the plasma was increased suggesting E2 functions to inhibit TGF- β 1 maturation. A change in TGF- β 1 in the plasma caused by E2 deficiency could alter the regulation of TGF- β 1 signaling pathways during cardiac development. Differences in the spatio-temporal expression of E2 and E1 during development could account for the different cardiac anomalies in the *E2^{-/-}* and *E1^{-/-}* mice.

In addition, while the cardiac anomalies in the *E2^{-/-}* mice are relatively mild, studies in patients with congenital defects similar to the *E2^{-/-}* mice indicate these patients are predisposed to cardiac and vascular disease [57-60], and need to be monitored on a regular basis throughout their lifetime. Several studies in mice reported that E2 is differentially expressed in right ventricular tissue [11,24], and E2 expression is increased in cardiac extracellular matrix in isoproterenol-induced hypertrophy [61]. Thus, in *E2^{-/-}* mice, older mice or in models of heart disease, such isoproterenol-induced hypertrophy [61] and myocardial infarction, function may be severely compromised.

Limitations of Study

This study has not determined the spatial and temporal expression of E2 and TGF- β 1 in cardiac development and will require the identification of E2 expression during embryonic development. Another limitation of the study is that long-term survival of *E2^{-/-}* mice was not defined. Development of a mouse model that mimics the deletion of E2 in 18p patients will be important to investigate survival and response to chronic cardiac disease in these subjects.

Conclusions

This study indicates E2 plays a role in cardiac development with over half the *E2^{-/-}* mice exhibiting VSDs and twenty percent with vessel anomalies. We did not detect abnormal vessel structure in *E2^{-/-}* mice, but did find that E2 deficiency inhibits stem cell mobilization.

Acknowledgments

This study was funded by grants from the National Institutes of Health, National Heart, Lung, and Blood Institute, R01HL065204 and R01HL17964 (JHP), American Heart Association, 11POST7600011 (AG), University Grants Commission, Bahadur Shah Zafar Marg, New Delhi-110 002, India (DS), American Heart Association, 09BGIA2050157 and 12SDG9050018 (YG), Natural Sciences and Engineering Council of Canada, NSERC RGPIN 355710 (ECD), and National Institutes of Health, National Heart, Lung, and Blood Institute, R01HL126747 (MWJ). We thank Lea-Jeanne Ringuette for technical assistance with the electron microscopy, and the Facility for Electron Microscopy Research at McGill University.

References

1. Turleau C (2008) Monosomy 18p. *Orphanet J Rare Dis* 3: 4.
2. Leimeister C, Steidl C, Schumacher N, Erhard S, and Gessler M (2002) Developmental expression and biochemical characterization of Emu family members. *Dev Biol* 249: 204-218.
3. Hasi-Zogaj M, Sebold C, Heard P, Carter E, Soileau B, et al. (2015) A review of 18p deletions. *Am J Med Genet C Semin Med Genet* 169: 251-264.
4. Xie CH, Yang, JB, Gong, FQ, Zhao ZY (2008) Patent ductus arteriosus and pulmonary valve stenosis in a patient with 18p deletion syndrome. *Yonsei Med J* 49: 500-502.
5. Movahhedian HR, Kane HA, Borgaonkar D, McDermott M, Septimus S (1991) Heart disease associated with deletion of the short arm of chromosome 18. *Del Med J* 63, 285-289
6. Digilio MC, Marino B, Giannotti A, Di Donato R, Dallapiccola B (2000) Heterotaxy with left atrial isomerism in a patient with deletion 18p. *Am J Med Genet* 94:198-200.
7. Schmidt B, Udink ten Cate F, Weiss M, Koehler U (2012) Cardiac malformation of partial trisomy 7p/monosomy 18p and partial trisomy 18p/monosomy 7p in siblings as a result of reciprocal unbalanced malsegregation--and review of the literature. *Eur J Pediatr* 171: 1047-1053.
8. Pearl W (1989) Heart disease associated with deletion of the short arm of chromosome 18. *Pediatr Cardiol* 10: 174-176.
9. Yi Z, Yingjun X, Yongzhen C, Liangying Z, Meijiao S, Baojiang C (2014) Prenatal diagnosis of pure partial monosomy 18p associated with holoprosencephaly and congenital heart defects. *Gene* 533, 565-569.
10. Bhattacharya JJ, Luo CB, Alvarez H, Rodesch G, Pongpech S, et al. (2004) PHACES syndrome: a review of eight previously unreported cases with late arterial occlusions. *Neuroradiology* 46: 227-233.
11. Kahr PC, Piccini I, Fabritz L, Greber B, Schöler H, et al. (2011) Systematic analysis of gene expression differences between left and right atria in different mouse strains and in human atrial tissue. *PLoS One* 6: e26389.
12. Bayer ML, Frommelt PC, Blei F, Breur JM, Cordisco MR, et al. (2013) Congenital cardiac, aortic arch, and vascular bed anomalies in PHACE syndrome (from the International PHACE Syndrome Registry). *Am J Cardiol* 112: 1948-1952.
13. Siegel DH, Shieh JT, Kwon EK, Baselga E, Blei F, et al. (2013) Copy number variation analysis in 98 individuals with PHACE syndrome. *J Invest Dermatol* 133: 677-684.
14. Xia Y, Hong H, Ye L, Wang Y, Chen H, et al. (2013) Label-free quantitative proteomic analysis of right ventricular remodeling in infant Tetralogy of Fallot patients. *J Proteomics* 84: 78-91.
15. Sasahara A, Kasuya H, Akagawa H, Ujiie H, Kubo O, et al. (2007) Increased expression of ephrin A1 in brain arteriovenous malformation: DNA microarray analysis. *Neurosurg Rev* 30, 299-305.
16. Gripp KW, Wotton D, Edwards MC, Roessler E, Ades L, et al. (2000) Mutations in TGIF cause holoprosencephaly and link NODAL signalling to human neural axis determination. *Nat Genet* 25: 205-208.
17. Overhauser J, Mitchell HF, Zackai EH, Tick DB, Rojas K, et al. (1995) Physical mapping of the holoprosencephaly critical region in 18p11.3. *Am J Hum Genet* 57: 1080-1085.
18. Klein C, Page CE, LeWitt P, Gordon MF, de Leon D, et al. (1999) Genetic analysis of three patients with an 18p- syndrome and dystonia. *Neurology* 52: 649-651.
19. Lemmers RJ, van den Boogaard ML, van der Vliet PJ, Donlin-Smith CM, Nations SP, et al. (2015) Hemizygoty for SMCHD1 in Facioscapulohumeral Muscular Dystrophy Type 2: Consequences for 18p Deletion Syndrome. *Hum Mutat* 36: 679-683.
20. Martinez-Mir A, Zlotogorski A, Gordon D, Petukhova L, Mo J, et al. (2007) Genomewide scan for linkage reveals evidence of several susceptibility loci for alopecia areata. *Am J Hum Genet* 80: 316-328.
21. Braghetta P, Ferrari A, De Gemmis P, Zanetti M, Volpin D, et al. (2004) Overlapping, complementary and site-specific expression pattern of genes of the EMILIN/Multimerin family. *Matrix Biol* 22: 549-556.
22. Doliana R, Bot S, Munguerra G, Canton A, Cilli SP, et al. (2001) Isolation and characterization of EMILIN-2, a new component of the growing EMILINs family and a member of the EMI domain-containing superfamily. *J Biol Chem* 276: 12003-12011.
23. Milanetto M, Tiso N, Braghetta P, Volpin D, Argenton F, et al. (2008) Emilin genes are duplicated and dynamically expressed during zebra fish embryonic development. *Dev Dyn* 237: 222-232.
24. Remme CA, Scicluna BP, Verkerk AO, Amin AS, van Brunschot S, et al. (2009) Genetically determined differences in sodium current characteristics modulate conduction disease severity in mice with cardiac sodium channelopathy. *Circ Res* 104: 1283-1292.
25. Colombatti A, Spessotto P, Doliana R, Mongiat M, Bressan GM, et al. (2011) The EMILIN/Multimerin family. *Front Immunol* 2: 93.
26. Bot S, Andreuzzi E, Capuano A, Schiavinato A, Colombatti A, et al. (2015) Multiple-interactions among EMILIN1 and EMILIN2 N- and C-terminal domains. *Matrix Biol* 41: 44-55.
27. Sa Q, Hoover-Plow JL (2011) EMILIN2 (Elastin microfibril interface located protein), potential modifier of thrombosis. *Thromb J* 9: 9.
28. Angel PM, Nusinow D, Brown CB, Violette K, Barnett JV, et al. (2011) Networked-based characterization of extracellular matrix proteins from adult mouse pulmonary and aortic valves. *J Proteome Res* 10: 812-823.
29. Votteler M, Berrio DA, Horke A, Sabatier L, Reinhardt DP, et al. (2013) Elastogenesis at the onset of human cardiac valve development. *Development* 140: 2345-2353.
30. Munjal C, Opoka AM, Osinska H, James JF, Bressan GM, et al. (2014) TGF-beta mediates early angiogenesis and latent fibrosis in an Emilin1-deficient mouse model of aortic valve disease. *Dis Model Mech* 7: 987-996.
31. Huang M, Sannanigaiah D, Zhao N, Gong Y, Grondolsky J, et al. (2015) EMILIN2 regulates platelet activation, thrombus formation, and clot retraction. *PLoS One* 10: e0115284.
32. Karunamuni G, Gu S, Doughman YQ, Noonan AI, Rollins AM, et al. (2015) Using optical coherence tomography to rapidly phenotype and quantify congenital heart defects associated with prenatal alcohol exposure. *Dev Dyn* 244: 607-618.
33. Jenkins MW, Watanabe M, Rollins AM (2012) Longitudinal Imaging of Heart Development with Optical Coherence Tomography. *IEEE J Sel Top Quantum Electron* 18: 1166-1175.
34. Coram RJ, Stillwagon SJ, Guggilam A, Jenkins MW, Swanson MS, et al. (2015) Muscledblind-like 1 is required for normal heart valve development in vivo. *BMC Dev Biol* 15: 36.
35. Karunamuni G, Gu S, Doughman YQ, Peterson LM, Mai K, et al. (2014) Ethanol exposure alters early cardiac function in the looping heart: a mechanism for congenital heart defects? *Am J Physiol Heart Circ Physiol* 306: H414-421.
36. Sivaguru M, Fried G, Sivaguru BS, Sivaguru VA, Lu X, et al. (2015) Cardiac muscle organization revealed in 3-D by imaging whole-mount mouse hearts using two-photon fluorescence and confocal microscopy. *Biotechniques* 59: 295-308.
37. Susaki EA, Tainaka K, Perrin D, Yukinaga H, Kuno A, et al. (2015) Advanced CUBIC protocols for whole-brain and whole-body clearing and imaging. *Nat Protoc* 10: 1709-1727.
38. Susaki EA, Tainaka K, Perrin D, Kishino F, Tawara T, et al. (2014) Whole-brain imaging with single-cell resolution using chemical cocktails and computational analysis. *Cell* 157: 726-739.
39. Hu Z, Rollins AM (2007) Fourier domain optical coherence tomography with a linear-in-wavenumber spectrometer. *Opt Lett* 32: 3525-3527.
40. Zanetti M, Braghetta P, Sabatelli P, Mura I, Doliana R, et al. (2004) EMILIN-1 deficiency induces elastogenesis and vascular cell defects. *Mol Cell Biol* 24: 638-650.
41. Davis EC (1993) Endothelial cell connecting filaments anchor endothelial cells to the subjacent elastic lamina in the developing aortic intima of the mouse. *Cell Tissue Res* 272: 211-219.
42. Davis EC (1993) Smooth muscle cell to elastic lamina connections in developing mouse aorta. Role in aortic medial organization. *Lab Invest* 68: 89-99.

43. Davis EC (1993) Stability of elastin in the developing mouse aorta: a quantitative radioautographic study. *Histochemistry* 100: 17-26.
44. Wagenseil JE, Mecham RP (2009) Vascular extracellular matrix and arterial mechanics. *Physiol Rev* 89: 957-989.
45. Dünker N, Kriegelstein K (2000) Targeted mutations of transforming growth factor-beta genes reveal important roles in mouse development and adult homeostasis. *Eur J Biochem* 267: 6982-6988.
46. Hao J, Ju H, Zhao S, Junaid A, Scammell-La Fleur T, et al. (1999) Elevation of expression of Smads 2, 3, and 4, decorin and TGF-beta in the chronic phase of myocardial infarct scar healing. *J Mol Cell Cardiol* 31: 667-678.
47. Van Hoof D, Dormeyer W, Braam SR, Passier R, Monshouwer-Kloots J (2010) Identification of cell surface proteins for antibody-based selection of human embryonic stem cell-derived cardiomyocytes. *J Proteome Res* 9: 1610-1618.
48. Gong Y, Zhao Y, Li Y, Fan Y, Hoover-Plow J (2014) Plasminogen regulates cardiac repair after myocardial infarction through its noncanonical function in stem cell homing to the infarcted heart. *J Am Coll Cardiol* 63: 2862-2872.
49. Brade T, Pane LS, Moretti A, Chien KR, Laugwitz KL (2013) Embryonic heart progenitors and cardiogenesis. *Cold Spring Harb Perspect Med* 3: a013847.
50. Sanford LP, Ormsby I, Gittenberger-de Groot AC, Sariola H, Friedman R, et al. (1997) TGFbeta2 knockout mice have multiple developmental defects that are non-overlapping with other TGFbeta knockout phenotypes. *Development* 124: 2659-2670.
51. Doetschman T, Barnett JV, Runyan RB, Camenisch TD, Heimark RL, et al. (2012) Transforming growth factor beta signalling in adult cardiovascular diseases and repair. *Cell Tissue Res* 347: 203-223.
52. Goumans MJ, Lebrin F, Valdimarsdottir G (2003) Controlling the angiogenic switch: a balance between two distinct TGF-b receptor signaling pathways. *Trends Cardiovasc Med* 13: 301-307.
53. Azhar M, Brown K, Gard C, Chen H, Rajan S, et al. (2011) Transforming growth factor Beta2 is required for valve remodeling during heart development. *Dev Dyn* 240: 2127-2141.
54. Galvin KM, Donovan MJ, Lynch CA, Meyer RI, Paul RJ, et al. (2000) A role for smad6 in development and homeostasis of the cardiovascular system. *Nat Genet* 24: 171-174.
55. Zacchigna L, Vecchione C, Notte A, Cordenonsi M, Dupont S, et al. (2006) Emilin1 links TGF-beta maturation to blood pressure homeostasis. *Cell* 124: 929-942.
56. Litteri G, Carnevale D, D'Urso A, Cifelli G, Braghetta P, et al. (2012) Vascular smooth muscle Emilin-1 is a regulator of arteriolar myogenic response and blood pressure. *Arterioscler Thromb Vasc Biol* 32: 2178-2184.
57. Hamirani YS, Dietl CA, Voyles W, Peralta M, Begay D, et al. (2012) Acute aortic regurgitation. *Circulation* 126: 1121-1126.
58. Nemer M (2008) Genetic insights into normal and abnormal heart development. *Cardiovasc Pathol* 17: 48-54.
59. Markwald RR, Norris RA, Moreno-Rodriguez R, Levine RA (2010) Developmental basis of adult cardiovascular diseases: valvular heart diseases. *Ann N Y Acad Sci* 1188: 177-183.
60. Force T, Bonow RO, Houser SR, Solaro RJ, Hershberger RE, et al. (2010) Research priorities in hypertrophic cardiomyopathy: report of a Working Group of the National Heart, Lung, and Blood Institute. *Circulation* 122: 1130-1133.
61. Molojavji A, Lindecke A, Raupach A, Moellendorf S, Köhrer K, et al. (2010) Myoglobin-deficient mice activate a distinct cardiac gene expression program in response to isoproterenol-induced hypertrophy. *Physiol Genomics* 41: 137-145.

Author Affiliations

[Top](#)

¹Department of Cellular and Molecular Medicine, Cleveland Clinic Lerner Research Institute, Cleveland, Ohio, USA

²Department of Molecular Cardiology, Cleveland Clinic Lerner Research Institute, Cleveland, Ohio, USA

³Department of Anatomy and Cell Biology, McGill University, Montreal, Quebec, Canada

⁴Department of Pediatrics and Division of Pediatric Cardiology, Case Western Reserve University School of Medicine, Cleveland, OH, USA

⁵Department of Studies and Research in Biochemistry and Centre for Bioscience and Innovation, Tumkur University, Tumkur- 572103, India

⁶Perelman School of Medicine, University of Pennsylvania, Division of Translational Medicine and Human Genetics, 3400 Civic Center Blvd., Bldg. 421 Philadelphia, PA 19104, USA

⁷Department of Radiation Oncology, University of Pennsylvania School of Medicine, Philadelphia, PA, USA

Submit your next manuscript and get advantages of SciTechnol submissions

- ❖ 80 Journals
- ❖ 21 Day rapid review process
- ❖ 3000 Editorial team
- ❖ 5 Million readers
- ❖ More than 5000 
- ❖ Quality and quick review processing through Editorial Manager System

Submit your next manuscript at • www.scitechnol.com/submission